Expansivity and heat capacity data for Lu and Sc crystals from 1 to 300 K: Spin-fluctuation and electron-phonon effects

C. A. Swenson
Ames Laboratory and Department of Physics and Astronomy, Iowa State University, Ames, Iowa 50011
(Received 27 March 1995)

Linear thermal expansivity (α) measurements from 1 to 300 K and heat capacity (C_p) measurements from 1 to 110 K are reported for single crystals of the hexagonal scandium and lutetium metals; the C_p data were combined with previous data to obtain smooth representations to 305 K for Lu and 350 K for Sc. The Θ_0's (352 and 190 K, respectively, for Sc and Lu) and γ's (10.38 and 8.30 mJ/mol K^2, respectively for Sc and Lu) are in reasonable agreement with previous data of various kinds. Electronic contributions are much larger for the α's than for the C_p's, with the large anisotropies of the α's primarily electronic in origin. The equivalent Debye Θ's for the lattice C_p's and the Grüneisen parameters Γ for the lattice α's both show an unexpected T dependence at "high" T ($T \gtrsim \Theta_0/2$), which can be associated with the disappearance of spin-fluctuation and electron-phonon enhancements to the electronic properties; this effect has been reported previously for Sc C_v's by Pleschiutschnig *et al.* [Phys. Rev. B **44**, 6794 (1991)]. While the resulting high-temperature "bare" or "density of states" γ for Sc, $\gamma_b = 5.75(25)$ mJ/mol K^2, is slightly larger than that calculated recently by Götz and Winter [J. Phys. Condens. Matter **5**, 1721 (1993)], the magnitude of the sum ($\gamma_{\rm spin} + \gamma_{ep}$) agrees well. For Lu, for which no recent calculations exist, $\gamma_b = 5.50(25)$ mJ/mol K^2. The various Γ's (a and c axis, lattice, and electronic) generally are quite anisotropic, with no obvious correlation between high- and low-T behavior. The anisotropy in Γ which is associated with the enhancement (spin plus e-p) contribution is very large, with similar magnitudes for the c-axis values ($\sim$17), but + for Lu and − for Sc. A 186-at. ppm Fe impurity in the scandium crystals makes a significant contribution to all of the data below 3.5 K. The resulting impurity Γ's are very large and very anisotropic ($\Gamma_a^{\rm Fe} = -40$, $\Gamma_c^{\rm Fe} = 30$).

I. INTRODUCTION

The present heat capacity (C_p) and linear thermal expansivity [$\alpha = (\partial \ln L/\partial T)_P$] measurements on lutetium single crystals were made to obtain pure-metal reference data for similar measurements on single-crystal LuH(D)$_x$ alloys; the results of these alloy measurements will be published elsewhere.[1] The corresponding measurements on scandium single crystals were suggested by the calculation by Götz and Winter[2] of the low-temperature electronic C_p coefficient γ for scandium, since the fine structure in their density of states suggested a possibly large electronic contribution to the thermal expansivity. Gschneidner and his collaborators[3,4] have demonstrated through C_p measurements on extremely pure (ETP, or electrotransport purified) samples of rare-earth metals that small amounts of iron[5,6] (for Sc) and hydrogen[7] (for Lu), among other impurities, probably are responsible for the very large discrepancies among previously reported low-temperature C_p results. Their extensive discussion of previous results for Sc and Lu (Ref. 3) will not be repeated here. The agreement between the present C_p's and those for the ETP metals provides assurance that our α data represent an intrinsic property of the pure materials. Lu and Sc are hexagonal crystals, so α measurements must be performed on single crystals for each of the two symmetry directions.

The correlation of C_p and α data using the Grüneisen relationships requires the (T-dependent) bulk modulus for an isotropic material, and a complete set of elastic constants for an anisotropic crystal. Tonnies, Gschneidner, and Spedding[8] have reported the temperature dependence of the elastic constants, as well as the linear thermal expansion, for single-crystal Lu, while Greiner, Beaudry, and Smith[9] reported the (small) effect of hydrogen on the elastic properties of Lu. Fisher and Dever[10] have investigated the effects of both temperature and impurities on the elastic constants of Sc crystals, with results for the best samples consistent with recent room-temperature measurements by Leisure *et al.*[11] The present C_p data, which extend from 1 to 105 K, overlap with the 1–20 K results for ETP samples of both Lu (Refs. 3, 7, 12) and Sc.[3,5] Previously, Gerstein *et al.* (GTSS in the following) published careful C_p results for less pure (but well-characterized) Lu (6–300 K),[13] and Sc (6–350 K).[14]

Pleschiutschnig and his collaborators have used inelastic neutron scattering to study the lattice dynamics of Lu (Ref. 15) and Sc.[16] They compare their calculated C_v for Sc with the GTSS data[14] and suggest that the resulting differences are consistent with the assumption that the electronic C_p coefficient γ decreases with increasing temperature above 20 K, probably due to the disappearance of the spin-fluctuation contribution. Grimvall[17] comments that the electron-phonon (e-p) contribution to γ, γ_{ep}, and, presumably, the spin-fluctuation contribution, $\gamma_{\rm spin}$, should begin to disappear for $T \gtrsim \Theta/10$, in agreement with this observation. Ikeda *et al.*[18] have demonstrated in 1–20 K C_p measurements that the spin fluctuations in Sc are quenched by 10 T magnetic fields, while Stierman *et al.*[19] also have studied spin fluctuations in single-crystal Sc using magnetic susceptibility measurements. These data show a maximum in the susceptibilities of the crystals near 30 K (approximately $\Theta/10$) and unusual magnetic behavior at lower temperatures (more significant for the c axis than for the a axis) which could be associated

with the onset upon cooling of spin fluctuations. Similar studies have not been reported for Lu.

The analysis of the present C_p and α data for Lu and Sc single crystals in terms of equivalent Debye Θ's and anisotropic Grüneisen parameters Γ supports Pleschiutschnig *et al.*'s suggestion that γ is temperature dependent for Sc,[16] extends it to include thermal expansivity effects, and shows similar behavior for Lu.

II. EXPERIMENTAL DETAILS

A. Sample preparation

Gschneidner[4] has discussed in detail the production of high-purity rare-earth (RE) metals. The initial Lu metal for the present samples was similar in quality to the starting material used by Thome and co-workers,[3,12] with hydrogen, nitrogen, oxygen, and carbon the major impurities. This also was the case for the initial Sc metal, except that subsequent analysis of the single-crystal material showed 186 at. ppm of Fe as the major impurity. For both metals, the preparation of single-crystal samples by a long-term anneal near the melting point (1500 °C for Lu, 1300 °C for Sc) in 10^{-8} Torr reduced the hydrogen content to less than 0.02 at. % (200 at. ppm).

The Lu α's were determined using two oriented single crystals [b (basal plane, referred to as a axis in the following) and c (symmetry) axis, each approximately 4 g and $6\times6\times12$ mm^3], which subsequently were alloyed with H(D) for the alloy studies. C_p data initially were obtained for these crystals, but the results which are used in this paper are for a third (a axis, 8.9 g, 0.051 mol) crystal, for which the data are consistent with the earlier results, but are more extensive. The two oriented Sc crystals were identical in orientation and similar in size to the original Lu crystals, with a combined mass of 2.5 g (0.05 mol).

B. Calorimetry, dilatometry

Heat capacities were measured from 1 to 110 K using a conventional heat-pulse calorimeter with Apiezon-N grease providing contact between the sample and the copper tray. A single locally calibrated[20] germanium resistance thermometer was used for temperature measurements. A mechanical heat switch provided thermal contact between the tray and an isothermal shield; no exchange gas was used at any time to cool the sample. For the Lu and Sc pure-crystal data, the ratio of the sample heat capacity to that of the addenda was approximately unity at all temperatures. The precision of the data (from the residuals of fits of power series to the data) is better than 0.3% at all temperatures, while the accuracy [from comparisons with data for copper[21] below 20 K and with the GTSS[13,14] data above 20 K] is $\pm0.5\%$ to 40 K, increasing to $+1.0(5)\%$ (C_p's systematically high) at 105 K. The ETP results of Thome[12] for Lu and of Tsang, Gschneidner, and Schmidt[5] for Sc, which were obtained using a common calorimeter, are systematically 2(1)% greater than the corresponding present results from 6 to 20 K; below 6 K, these differences for both Lu and Sc are similar to the differences between Thome's data and the present data for pure copper. These differences could, for instance, arise from small differences in thermometry. Atomic weights and densities are from the summary by Gschneidner.[22]

The linear thermal expansivities $[\alpha=(1/L)(\Delta L/\Delta T)=(\partial \ln L/\partial T)_P$ for small $\Delta L]$ of these 12-mm-long single crystals were determined from 1 to 300 K using a variable-sample-length differential capacitance dilatometer.[23] All data were taken isothermally (T constant to 0.001 K); capacitance readings subsequent to a change in T (which could be as small as ±0.5 K or as large as ±20 K) were taken only after capacitance drift (presumably due to T differences between the sample and the dilatometer) was negligible. The absolute accuracy of these measurements varies from the larger of $\pm1.5\times10^{-9}$/K ($T<6$ K for c-axis samples, <9 K for Sc a-axis samples, <20 K for Lu a-axis samples) to $\pm0.5\%$ at higher temperatures. The internal consistency of the data (the larger of $\pm5\times10^{-10}$/K or $\pm0.2\%$) is much better than this for a given run, with the magnitude of the correction for the cell ''expansion'' a major source of systematic uncertainty.

C. Data analysis

Barron and Morrison[24] have shown that low-temperature C_p data for a pure metal can be represented rigorously by a power series which contains only odd powers of T; this relation can be written in the useful C_p/T vs T^2 form as

$$C_p/T=\sum_{n=0}^{N} C_n T^{2n}. \tag{1a}$$

Similar considerations[25] give the low-temperature thermal expansivities for a pure metal as

$$\alpha/T=\sum_{n=0}^{N} A_n T^{2n}. \tag{1b}$$

For a pure nonmagnetic metal, the first term in Eqs. (1) is associated with electronic contributions (for C_p, $C_0=\gamma$), while the higher-order terms are associated with lattice contributions. The second term in Eq. (1a) ($n=1$) gives the limiting ($T=0$) form of the lattice C_p, with the Debye temperature Θ_0 given by

$$\Theta_0=[1.944\times10^6 \ \ (\text{mJ/g mol K})/C_1]^{1/3} \ \ \text{K}. \tag{2}$$

The significances of the lead terms for the α expression [Eq. (1b)] are more complex than for C_p, and will be discussed in a later section.

When impurities are present (as for Sc), the above discussion may not be valid, and the uniqueness of the first two terms in Eqs. (1) (the extrapolation to $T=0$) should be tested using a range of minimum and maximum temperatures for the fits. The contributions of the higher-order terms in Eq. (1) must be recognized to obtain meaningful values of C_0 (γ) and C_1 (Θ_0). For Lu, the magnitude of these terms [$n>1$, Eq. (1a)] is 0.5% at 2.6 K, 5% at 5 K, and 8% at 6 K, so a linear C_p/T vs T^2 relation cannot be used even at ''low'' temperatures. The present Sc data (both C_p and α) show a pronounced impurity contribution below 3.5 K, but, fortunately, the effects of the higher-order ($n>1$) terms in Eqs. (1) are much smaller for Sc than for Lu, with plots of C_p/T and α/T vs T^2 linear from 4 to 10 K ($16\leqslant T^2\leqslant100$), so the effect of the excess low-temperature C_p is minimized for the data analysis. The impurity contribution can be represented

by the limiting high-temperature form of a Schottky function, so additional terms (C_{-2}/T and A_{-2}/T^2) must be added to the low-temperature representations of C_p and α, respectively.

Higher-temperature (more slowly varying) C_p and α data can be represented more easily by a power series in T:

$$C_p = \sum_{n=0}^{N} C_n T^n \tag{3a}$$

and

$$\alpha = \sum_{n=0}^{N} A_n T^n. \tag{3b}$$

For precise data, least-squares fits of Eqs. (3) often are used for two or more overlapping temperature ranges to avoid an excessive number of terms; none of the least-squares-determined parameters has any physical significance.

Experimental data $C_p(T_i)$ (where T_i represents an individual data point) can be presented quite sensitively for a wide range of temperatures using temperature-dependent equivalent Debye Θ's to represent parametrically the lattice contribution $C_p^{\rm lat}(T_i)$. $\Theta(T_i)$ is defined by the relation

$$C_p^{\rm lat}(T_i) = C_p(T_i) - C_p^{\rm elect} = C_p - \gamma T_i = C_D[T_i/\Theta(T_i)], \tag{4}$$

where $C_D(T/\Theta)$ is the Debye function.[26] $\gamma\,(C_0)$ is obtained from a fit of Eq. (1a) to the low-temperature data, which also gives C_1 and, hence, Θ_0 [Eq. (2)]. For a Debye solid, $\Theta(T_i)=\Theta_0$, while for a real solid Θ usually decreases to a minimum with increasing T and then varies only slowly with temperature.

The constant-volume heat capacity C_v is required for comparison with theoretical calculations, such as those related to lattice dynamics studies. The relationship between C_p and C_v is given by

$$C_v = C_p/\{1+[\beta^2 B_S T/(C_p/V)]\}, \tag{5}$$

where β $[=(\partial \ln V/\partial T)_p]$ is the volume thermal expansivity, B_S is the adiabatic bulk modulus, and C_p/V is the heat capacity per unit volume.

The thermal expansivities and heat capacities have a common origin, since each is obtained from a derivative of the entropy. When C_p and α can be expressed as the sum of ''independent'' contributions [as for a metal; Eqs. (1)], this relationship will be different for each contribution. The Grüneisen model assumes that the entropy $S(V,T)$ for each contribution can be described by a characteristic temperature (energy) $\Phi^i(V)$ as $S^i(V,T)=S^i[\Phi^i(V)/T]$.[25] The volume thermal expansivity β_i and C_p^i are related through the dimensionless volume Grüneisen parameter,

$$\Gamma_v^i = \beta^i B_S/(C_p^i/V) = -d\ln\Phi^i/d\ln V, \tag{6a}$$

where the parameters are as in Eq. (5). The magnitude of Γ usually is less than 4; its sign may be + or −.[25] Γ_v^i gives the volume dependence of the characteristic energy.

For a nonmagnetic metal, independent Γ_v's will be defined for the electronic ($\Gamma_v^{\rm elect}$) and lattice ($\Gamma_v^{\rm lat}$) contributions; for scandium, a third, anomalous, contribution ($\Gamma_v^{\rm an}$) will exist. The characteristic electronic energy $\Phi^{\rm elect}$ is inversely proportional to the density of states at the Fermi level, $n(\epsilon_F)$, so

$$\Gamma_v^{\rm elect} = d\ln[n(\epsilon_F)]/d\ln V. \tag{6b}$$

For the lattice, the characteristic energy at $T=0$ is the Debye temperature, Θ_0, and

$$\Gamma_v^{\rm lat} = -d\ln\Theta_0/d\ln V. \tag{6c}$$

The significance of $\Gamma_v^{\rm lat}$ is more complex at higher T's.[25]

For a single crystal, the volume and linear expansivities are related by

$$\beta^i = \alpha_a^i + \alpha_b^i + \alpha_c^i. \tag{7a}$$

The α^i are identical for an isotropic material ($\beta^i=3\alpha^i$), while for a crystal with axial symmetry (such as the hexagonal metals Sc and Lu), $\alpha_a=\alpha_b$, and

$$\beta^i = 2\alpha_a^i + \alpha_c^i. \tag{7b}$$

Equation (6a) remains valid for the general case, but the usually different thermal expansivities for the individual symmetry directions can be used to obtain additional information. For hexagonal symmetry, the relations equivalent to Eq. (6a) become[25]

$$\Gamma_a^i = (V/C_p^i)[(C_{11}+C_{12})\alpha_a^i + C_{13}\alpha_c^i] = -[\partial\ln\Phi^i(a,c)/\partial\ln a]_c, \tag{8a}$$

$$\Gamma_c^i = (V/C_p^i)[(2C_{13}\alpha_a^i + C_{12}\alpha_c^i] = -[\partial\ln\Phi^i(a,c)/\partial\ln c]_{a,b}, \tag{8b}$$

where the C_{ij}'s are the elastic constants, and the Γ's now give the strain dependences of the characteristic energies. The electronic and lattice Γ's follow by analogy with Eqs. (6b) and (6c). The inverse relationships, which demonstrate the importance of elastic coupling via C_{13} between the a- and c-axis α's, are[25]

$$\alpha_a^i = (C_p^i/VD)[C_{33}\Gamma_a^i - C_{13}\Gamma_c^i], \tag{9a}$$

$$\alpha_c^i = (C_p^i/VD)[(C_{11}+C_{12})\Gamma_c^i - 2C_{13}\Gamma_a^i], \tag{9b}$$

with

$$D = C_{33}(C_{11}+C_{12}) - 2(C_{13})^2.$$

III. RESULTS AND DISCUSSION

A. C_p and α data

Figures 1 and 2 give for both Lu and Sc the present C_p data to 40 K, and those[13,14] of GTSS for higher temperatures. The GTSS data show increasing scatter below 40 K, but join smoothly with the present data at that temperature. A C_p/T vs T representation is used in Fig. 1 to emphasize the relative magnitudes of the electronic contributions to C_p ($C_p^{\rm elect}/T$ = const); these are much smaller for C_p than for the α's (see the following). Figure 2 is of the form suggested by Eq. (1a), and shows the quite different effects of the higher-order terms for Sc and Lu; as well as the low-temperature, Fe-related ''anomaly'' for Sc. Table I contains the values of the

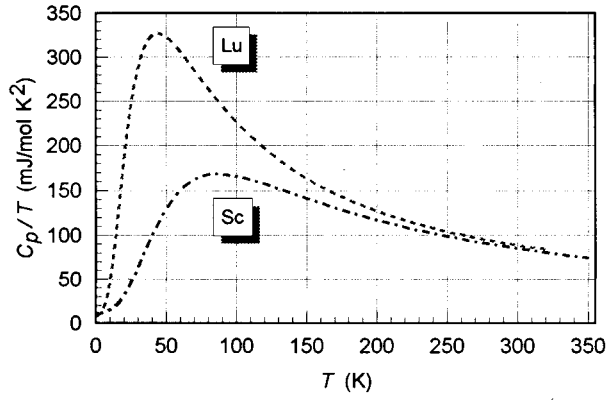

FIG. 1. C_p/T vs T representation of the smooth heat capacities of Sc and Lu, using Eqs. (1a) or (3a) and the parameters in Table I.

parameters for Eqs. (1a) or (3a) which are used to represent these data, with the C_{-2} term for Sc representing the anomaly contribution.

Figures 3–5 present the thermal expansivity results for both Lu and Sc. The volume thermal expansivity β in Fig. 3 is given by Eq. (7b). The corresponding relative expansions for Lu $[L(T)/L(293\ \mathrm{K})$, not shown] are consistent with those of Tonnies, Gschneidner, and Spedding.[8] Figure 4, which is of the same form as Fig. 1 for C_p, shows that electronic

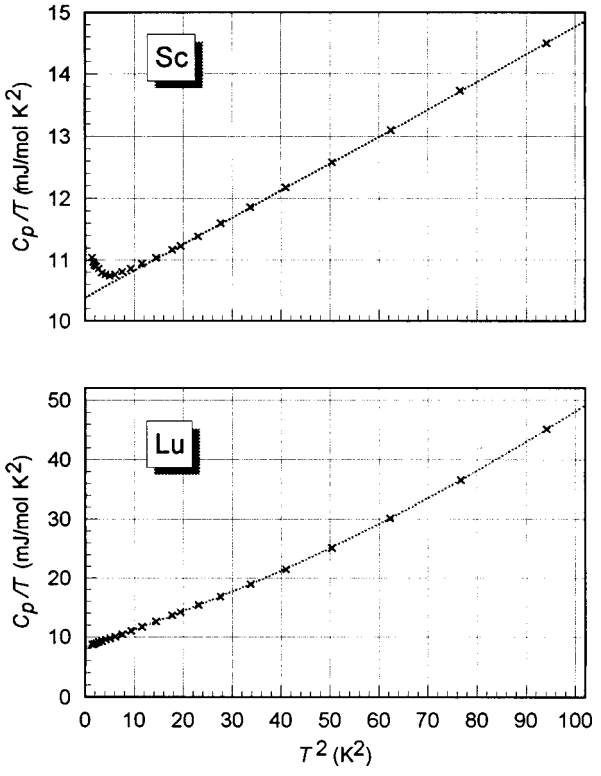

FIG. 2. C_p/T vs T^2 representation of the low-temperature C_p data for Sc and Lu; the symbols in each case correspond to the actual data, while the dotted lines are calculated from the pure-metal parameters in Table I. The zero for the Sc figure is suppressed; the vertical scale for Sc is a factor of 10 more sensitive than for Lu.

effects ($\alpha/T=$const) are of much greater relative importance for α than for C_p, and, in particular, that the anisotropy of the α's for Sc in Fig. 3 would be much larger without a large negative electronic contribution to α_c. Figure 5 presents the low-temperature results in the same form as Fig. 2 for C_p, with a corresponding "anomaly" contribution for Sc at low temperature. The *a*-axis Lu α's are very small at low T, with structure which may or may not have significance. Table II for Sc and Table III for Lu give the parameters for Eqs. (1b) and 3(b) which represent these results; the A_{-2} term for Sc represents the anomaly contribution.

The $T=0$ Debye temperature Θ_0 [Eq. (2)] is compared directly in Table IV with values from other C_p experiments and with those calculated from elastic-constant data and the analysis of inelastic neutron scattering dispersion relations. For consistency, a reanalysis of the ETP results is given which uses the same procedures which were used to obtain the smooth relations of Table I. The elastic-constant values were calculated from the data cited using procedures described by Grimvall,[27] while the neutron scattering values are found in the cited papers. The neutron values refer to 295 K dispersion relations, and should be increased by approximately 0.8% (Lu) and 0.6% (Sc) to obtain values corresponding to the $T=0$ volumes. Table IV also contains a comparison of the electronic C_p coefficients γ from the present experiments [C_0, Eq. (1a), in Table I] with those for the ETP samples, and for the calculation of Götz and Winter.[2] The differences in the C_p parameters for a common analysis undoubtedly reflect the systematic effects which were discussed in Sec. II B. These differences (except possibly for the theory) are not significant.

B. Spin and *e-p* effects; C_p

Figure 6 give the temperature dependences of the equivalent Debye Θ's for Sc and Lu [Eq. (4)], both for the actual data points and for the smooth representations of the C_p data. the present data are used for $T<40$ K, those[13,14] of GTSS for higher temperatures (Table I). Initially, a common structure appeared above 50 K which disappeared when the data were corrected to correspond to the most recent (International Temperature Scale of 1990, the ITS-90) temperature scale;[28] the platinum resistance thermometer which was used for both of these experiments was calibrated by the (then) National Bureau of Standards using the NBS-55 scale[29] from 12 to 90 K; and the ITS-48 at higher temperatures.[28,30] The smooth temperature dependence of C_v which is plotted for each metal illustrates the sensitivity of this representation, since at 300 K C_p is greater than C_v [Eq. (5)] by 1.12% for Lu and 0.93% for Sc.

A puzzling feature in Fig. 6 for both Sc and Lu is the *increase* in Θ with increasing T above roughly 50 K, since this corresponds to a decrease in C_{p}^{lat} relative to the Debye function. Barron, Collins, and White[25] imply that Θ should be independent of T above $0.4\Theta_0$, in agreement with calculations from neutron scattering dispersion relations[15,16] for which Θ approaches a constant value (Θ_∞) at high temperature (Table IV). The "C_p" relations in Fig. 6 were calculated using Eq. (4) and the γ's in Table IV. Pleschiutschnig *et al.*'s observation[16] that γ for Sc begins to decrease above 20 K suggests that this is not appropriate. For metals such as Sc

TABLE I. The parameters for Eqs. (1a) or (3a) which will reproduce the experimental C_p's for scandium and lutetium metals, in units of mJ/mol K. The final parameters in this table ($C_0^{\rm adj}=\gamma_b$) were used to obtain the electronic C_p's for the calculation of "high-T" lattice C_p's. See the text for details.

	Scandium				Lutetium			
Range	$1<T<27.5$ K	$27.5<T<40$ K	$40\leqslant T<105$ K	$105\leqslant T<350$ K	$T<7$ K	$7\leqslant T<40$ K	$40\leqslant T<104$ K	$104\leqslant T<305$ K
	Present data		Reference 14		Present data		Reference 13	
Eq.	(1a)	(3a)	(3a)	(3a)	(1a)	(3a)	(3a)	(3a)
C_{-2}[a]	1.4							
C_0	1.0380×10	3.1301×10^{3}	1.7707×10^{3}	-2.2490×10^{4}	8.2988	-7.1404×10^{2}	1.09913×10^{4}	1.8749×10^{3}
C_1	4.4501×10^{-2}	-3.5628×10^{2}	-1.9801×10^{2}	8.5020×10^{2}	2.8384×10^{-1}	3.7956×10^{2}	-2.20382×10^{3}	4.6840×10^{2}
C_2	-3.8811×10^{-5}	1.4284×10	6.9635	-7.4701	8.5707×10^{-4}	-7.3433×10	1.69389×10^{2}	-4.0734
C_3	4.2003×10^{-7}	-1.3821×10^{-1}	3.7610×10^{-2}	3.8960×10^{-2}	3.1102×10^{-6}	7.0373	-5.53099	1.8642×10^{-2}
C_4	-1.1045×10^{-9}	4.4544×10^{-4}	-1.8857×10^{-3}	-1.2075×10^{-4}		-2.8202×10^{-1}	1.05034×10^{-1}	-4.3201×10^{-5}
C_5	1.4115×10^{-12}		1.6013×10^{-5}	2.0506×10^{-7}		5.8541×10^{-3}	-1.24038×10^{-3}	4.0083×10^{-8}
C_6	-9.0105×10^{-16}		-4.4260×10^{-8}	-1.4651×10^{-10}		-6.2796×10^{-5}	8.99992×10^{-6}	
C_7	2.2816×10^{-19}					2.7686×10^{-7}	-3.67957×10^{-8}	
C_8							6.49262×10^{-11}	
$C_0^{\rm adj}$				5.75(25)				5.50(20)

[a]Impurity contribution, present samples only.

and Lu, the low-temperature γ consists of a "bare" density of states contribution (γ_b) which is enhanced by electron-phonon (γ_{ep}) and spin-fluctuation ($\gamma_{\rm spin}$) contributions;[2]

$$\gamma=\gamma_b+\gamma_{\rm spin}+\gamma_{ep}=\gamma_b(1+\lambda). \tag{10}$$

Grimvall[17] suggests, in agreement with Pleschiutschnig *et al.*'s observation,[16] that the electron-phonon (and spin-fluctuation) contributions should begin to decrease for $T\geqslant\Theta/10$, so it is reasonable to assume that the electronic C_p is given by γT near $T=0$, and by $\gamma_b T$ at "high" temperatures.

To test this postulate, $\Theta(T)$ for each metal was recalcu-

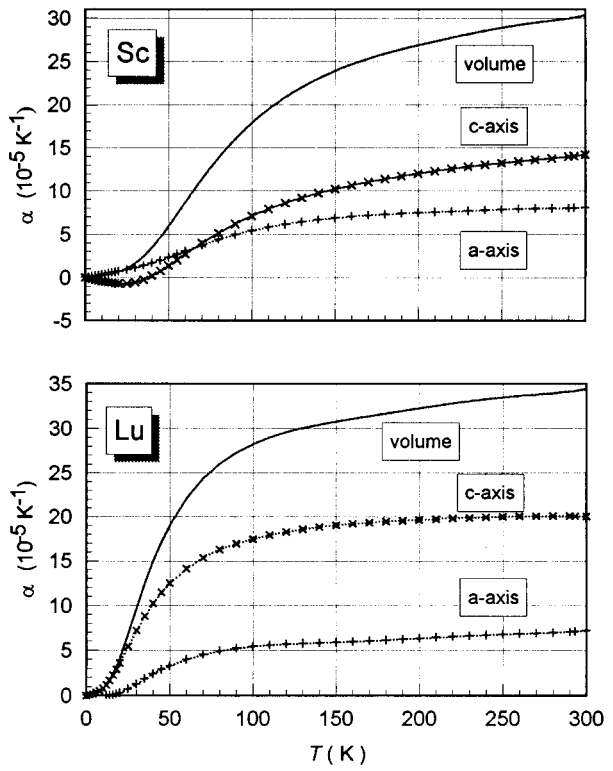

FIG. 3. The smooth thermal expansivities for Sc and Lu as calculated from the parameters in Tables II and III. The symbols indicate only the crystallographic orientation (+ for *a* axis, × for *c* axis).

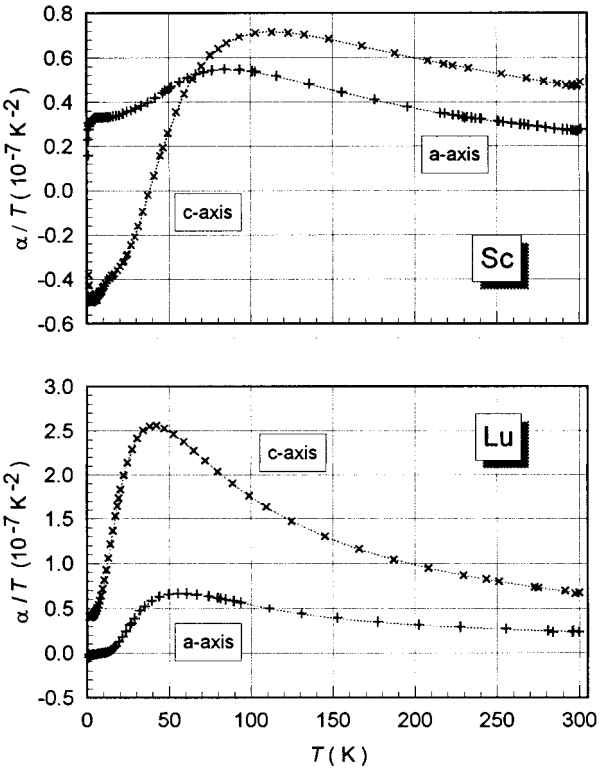

FIG. 4. α/T vs T representation of the expansivities for Sc and Lu; the symbols represent expansivity data, while the dotted lines are calculated from Eqs. (1b) or (3b) and the pure-metal parameters in Tables II and III.

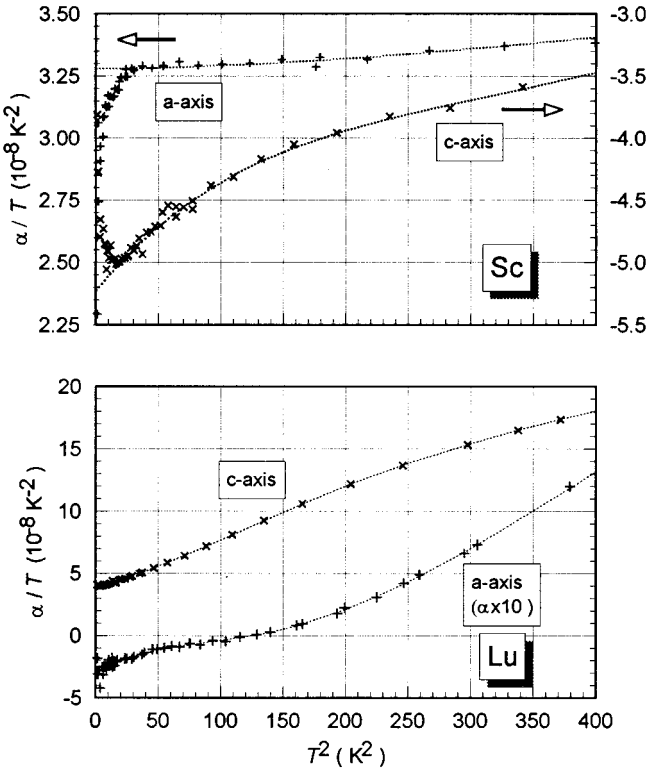

FIG. 5. α/T vs T^2 representation of the low-temperature expansivity data. See the caption for Fig. 4. For Sc, the *a*-axis scale is on the left, the *c*-axis scale (displaced, less sensitive, and with negative values) is on the right. For Lu, the *a*-axis α's, as indicated, have been multiplied by 10 before plotting.

lated for decreasing values of γ in Eq. (4) until Θ was constant above the minimum. The results of these calculations are shown by the lower ($C_v^{\rm adj}$) curves in Fig. 6, which follow from using $\gamma_b = C_0^{\rm adj} = 5.75$ (vs 10.38 at $T=0$) mJ/mol K^2 for Sc and 5.50 (vs 8.30 at $T=0$) mJ/mol K^2 for Lu (Table I). The symbols (+) in each case represent the actual data (converted to C_v) while the dotted line corresponds to the smooth relation which represents these data. The bracketing dashed lines illustrate uncertainties in γ_b of ± 0.25 and ± 0.20 mJ/mol K^2 for Sc and Lu, respectively. The sensitivity of this representation increases as T becomes greater than Θ; for Sc, $T=\Theta$ at 320 K, while for Lu, $T=\Theta$ at 160 K. The scatter in the data corresponds to approximately $\pm 0.2\%$ except at the highest temperatures. The resulting values for Θ_∞ are in excellent agreement with those from other experiments (see Table IV), including that from an energy-dispersive x-ray-diffraction experiment.[31] The dispersion relations for Lu (Ref. 15) show a minimum value $\Theta = 155.8$ K at 23 K and $\Theta_\infty = 159$ K. The high-temperature, explicit, anharmonic contribution to C_p (linear in T) should be small for these "low" ($T \approx \Theta$) temperatures.[25]

Götz and Winter[2] calculate $\gamma_b = 5.228$ mJ/mol K^2 [$n(\epsilon_F) = 30.18$ states/Ry at.] for Sc, roughly 10% smaller than that given by the present analysis [33.2(1.4) states/Ry at.]. Their calculation of $(\gamma_{\rm spin} + \gamma_{ep}) = 4.65$ mJ/mol K^2 is consistent with the present value, 4.63(25) mJ/mol K^2, which is calculated from

$$C_0 - C_0^{\rm adj} = \gamma - \gamma_b = \gamma_{\rm spin} + \gamma_{ep}\,. \tag{11}$$

The difference between their $\gamma = 0.89$ and the present $\gamma = 0.81(4)$ [Eq. (10)] reflects the differences in γ_b. For Lu, the present analysis gives $\gamma_b = 5.50(25)$ mJ/mol K^2 [$n(\epsilon_F) = 31.8(1.2)$ states/Ry at.], and $\lambda = 0.51(2)$, which implies smaller spin and/or *e-p* effects. No theoretical calculations exist for Lu which are equivalent to those by Götz and Winter for Sc. Tsang *et al.*[3] summarize theoretical density of states results for a number of rare-earth metals (as of 1984), together with estimates of the spin and *e-p* contributions. For Sc, the bare $n(\epsilon_F)$ summary is roughly in agreement with the above, while the *e-p* contribution appears to be underestimated, and that for spins overestimated. For Lu, their summary is consistent with $n(\epsilon_F) = 25(1)$ states/Ry at., and $\lambda = 0.95(5)$, although fewer studies are involved. The density of states relations for these metals show considerable structure,[2] so small shifts in the location of the Fermi level can have a large effect on $n(\epsilon_F)$.

C. Spin and *e-p* effects; α's and Γ's

Equations (8) were used to calculate the anisotropic Grüneisen parameters Γ for the Sc and Lu lattice and electronic contributions, as well as for the anomalous (impurity) contribution for Sc. The smooth representations of the data in Tables I–III were used for these calculations, as well as ana-

TABLE II. The parameters for Eqs. (1b) or (3b) which will reproduce the present experimental α's for pure lutetium metal, in units of K^{-1}. The final parameters in this table ($A_0^{\rm adj}$) were used to obtain electronic α's for the calculation of "high-T" lattice α's. See the text for details.

	Lutetium *a*-axis			Lutetium *c* axis		
Range	$1<T<11.9$ K	$11.9\leqslant T\leqslant 34$ K	$34<T<300$ K	$T\leqslant 18$ K	$18<T\leqslant 95$ K	$95<T<300$ K
Eq.	(1b)	(3b)	(3b)	(1b)	(3b)	(3b)
A_0	-2.500×10^{-9}	-1.9723×10^{-6}	-4.5495×10^{-6}	3.8230×10^{-8}	1.7032×10^{-6}	5.5577×10^{-6}
A_1	1.980×10^{-11}	5.9683×10^{-7}	2.5830×10^{-7}	2.8722×10^{-10}	-4.6123×10^{-7}	2.2003×10^{-7}
A_2		-7.0630×10^{-8}	-2.6307×10^{-9}	1.5226×10^{-12}	4.7697×10^{-8}	-1.3607×10^{-9}
A_3		4.0748×10^{-9}	1.3400×10^{-11}	-5.7851×10^{-15}	-1.2955×10^{-9}	3.9409×10^{-12}
A_4		-1.1869×10^{-10}	-3.3112×10^{-14}	6.0323×10^{-18}	1.7225×10^{-11}	-4.3746×10^{-15}
A_5		1.7576×10^{-12}	3.1834×10^{-17}		-1.1487×10^{-13}	
A_6		-1.0612×10^{-14}			3.0668×10^{-16}	
$A_0^{\rm adj}$			$5.0(5)\times10^{-9}$			$-0.3(2)\times10^{-9}$

TABLE III. The parameters for Eqs. (1b) or (3b) which will reproduce the present experimental α's for pure scandium metal, in units of K^{-1}. The final parameters in this table (A_0^{adj}) were used to obtain electronic α's for the calculation of "high-T" lattice α's. See the text for details.

	Scandium a axis			Scandium c axis	
Range	$T \leqslant 53$ K	$53 \leqslant T < 300$ K	$2 < T \leqslant 24.5$ K	$24.5 < T 56$ K	$56 \leqslant T < 300$ K
Eq.	(1b)	(3b)	(1b)	(3b)	(3b)
A_{-2}[a]	-3.9×10^{-8}		5.0×10^{-8}		
A_0	3.2779×10^{-8}	$6.552\,78\times10^{-6}$	-5.2287×10^{-8}	-3.9117×10^{-8}	-5.6057×10^{-6}
A_1	5.1753×10^{-13}	-4.678×10^{-7}	1.2226×10^{-10}	-5.3152×10^{-12}	1.0000×10^{-7}
A_2	9.2069×10^{-15}	$1.481\,85\times10^{-8}$	-4.2888×10^{-13}	5.3700×10^{-14}	1.6775×10^{-9}
A_3	-7.3457×10^{-18}	$-2.117\,22\times10^{-10}$	8.3826×10^{-16}	-3.2916×10^{-17}	-2.3982×10^{-11}
A_4	2.9095×10^{-21}	$1.746\,00\times10^{-12}$	-7.3648×10^{-19}	9.5888×10^{-21}	1.2744×10^{-13}
A_5	-5.6336×10^{-25}	$-8.799\,95\times10^{-15}$	2.4208×10^{-22}	-1.3967×10^{-24}	-3.1498×10^{-16}
A_6	4.1773×10^{-29}	$2.672\,31\times10^{-17}$		8.1095×10^{-29}	3.0118×10^{-19}
A_7		$-4.485\,44\times10^{-20}$			
A_8		$3.192\,27\times10^{-23}$			
A_0^{adj}		$-1.7(2)\times10^{-9}$			$2.0(2)\times10^{-8}$

[a]Impurity contribution, these samples only. See the text.

lytic representations of the elastic-constant results of Fisher and Dever[10] for Sc and Tonnies *et al.*[8] for Lu (see the Appendix). Figure 7 gives (in the dashed and dotted curves) the lattice Γ's which result when the low-temperature parameters [C_0 and A_0, Eqs. (1)] are used to define the electronic contributions to C_p and α, while the solid lines represent the corresponding Γ_v. The $T=0$ Γ^{elect}, as well as the $T=0$ and 300 K Γ^{lat}, are given in the upper part of Table V for both metals.

The lattice Γ's in Fig. 7 show the same type of high-temperature inconsistency which appears in Fig. 6 for C_p. Barron, Collins, and White[25] comment that lattice Γ's should become temperature independent for $T > \Theta/10$, which clearly is not the case, presumably because of the disappearance of spin and e-p contributions to α at high temperatures. The Γ's were recalculated using systematic iterations of A_0 [Eq. (1b)] for both crystal directions ($\alpha^{lat} = \alpha - A_0 T$), as well as γ_b (C_0^{adj}) to obtain lattice C_p's, until both Γ_a^{lat} and Γ_c^{lat} were temperature independent (minimum standard deviations) at "high" temperatures ($T > 140$ K for Sc, $T > 70$ K for Lu). Tables II and III contain the values of A_0 (A_0^{adj}) which resulted from this procedure; by analogy with the C_p discussion, the electronic contribution to α is given by $A_0 T$ at low T [the A_0 are those for Eq. (1b) in Tables II and III], and by $A_0^{adj} T$ at high T. Although the minimum in the standard deviation for the lattice Γ's was well defined, its breadth is reflected in the stated uncertainties.

The lower half of Table V summarizes the results for the "high-T" Γ's, with the Γ^{lat} also indicated in Fig. 7 as the "adjusted" symbols (○ for a axis, × for c axis). For Sc, the adjusted lattice Γ's are isotropic [$\Gamma_a^{lat} = \Gamma_c^{lat} = 0.86(2)$] and intermediate between the original values. For Lu, Γ_a^{lat} is un-

TABLE IV. A comparison of Debye Θ's and γ's from various experiments.

	Scandium	Lutetium	References
Θ_0 (K)			
C_p, crystals	352.2(10)	189.9(5)	Present data and analysis
C_p, ETP	345.3(10)	183.2(5)	Lu, Sc, Ref. 3
C_p, ETP	346.3(10)	190.3(3)	Ref. 3 data, present analysis
Elastic	356.5(10)	185.(10)	Sc, Refs. 10,11; Lu, Ref. 8
Elastic		186	Ref. 9
Neutron	354.2	188	Sc, Ref. 16; Lu, Ref. 15
γ (mJ/mol K^2)			
C_p, crystals	10.38	8.299	Present data and analysis
C_p, ETP	10.334(11)	8.194(16)	Ref. 3
C_p, ETP	10.33	8.305	Ref. 3 data, present analysis
Theory	9.88		Ref. 2
Θ_∞ (K)	$T > 140$ K	$T > 70$ K	
C_p, crystals	310.5(12)	157.5(10)	Present data and analysis
Neutron	310	159	Sc, Ref. 16; Lu, Ref. 15
X ray		157.(1)	Ref. 31
γ_b (mJ/mol K^2)	5.75(25)	5.50(20)	C_0^{adj}, Table I
Theory	5.23		Ref. 2

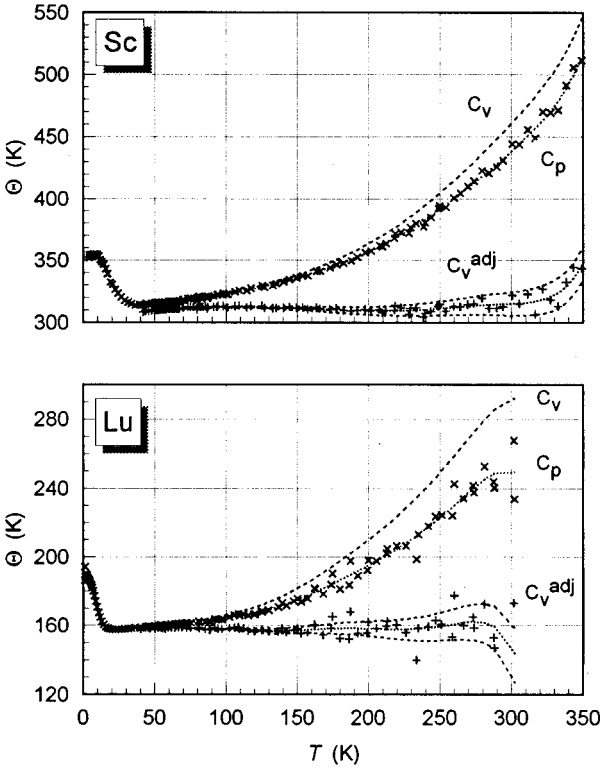

FIG. 6. Equivalent Debye Θ's for Sc and Lu lattice heat capacities. The upper curves in each figure use the $T=0$ value, γ, in Eq. (4), while the $C_v^{\rm adj}$ curves use γ_b. Note that Θ and C_v have an inverse relationship. See the text for details.

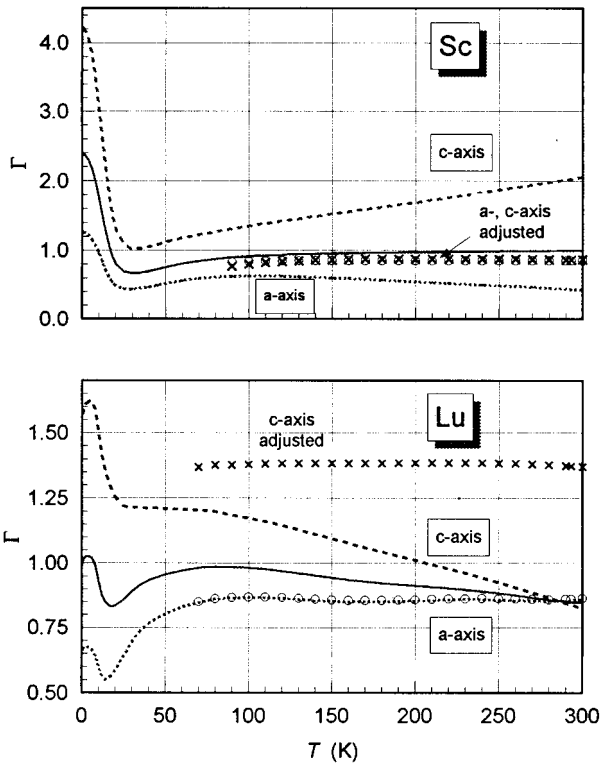

FIG. 7. Lattice Grüneisen parameters for Sc and Lu [Eqs. (8)], calculated from the smooth relations defined by Tables I–III and in the Appendix. The curves were calculated using low-temperature parameters (the solid lines represent the volume Grüneisen parameter) to obtain the electronic contribution, while the symbols (○ for *a* axis, × for *c* axis) use the adjusted (high-*T*) electronic parameters. See the text for details.

affected by the adjustment, while $\Gamma_c^{\rm lat}$ increases by 50% to 1.38. The $A_0^{\rm adj}$ and $C_0^{\rm adj}$ were used to calculate the "high-T" electronic Γ's which also are given in Table V, and which are characteristic of the bare density of states. These show a smaller anisotropy than those for $T=0$ (the enhanced values).

By analogy with Eq. (11), the combined spin and *e-p* contributions to the electronic α's are given by the difference between A_0 [Eq. (1b)] and $A_0^{\rm adj}$ for each of the crystallographic directions. These differences for Sc and Lu (and $\gamma-\gamma_b$) were used to calculate the Γ's which are given in Table V for the "high-T" "spin + *ep*" contribution. These Γ's are highly anisotropic for both Sc and Lu, with the largest magnitudes for the *c*-axis direction, but with little other similarity. Γ_c has different signs for the two metals (negative for Sc, positive for Lu), while the Γ_a's are positive for both, but with quite different magnitudes. As a result, Γ_v is small for Sc and large for Lu.

D. Impurity effects, Sc

The impurity (presumably 186 at. ppm of Fe) contributions to both C_p and the α's for Sc are large (Figs. 2 and 5), and are significant below approximately 3.5 K ($T^2=12$). They can be represented within experimental accuracy by terms proportional to T^{-2}, using the parameters in Tables I and III. The present C_p results are inconsistent with those of Tsang and Gschneidner[6] which show a much greater effect for samples with smaller concentrations of Fe. Indeed, the present C_p data resemble theirs for a 30 at. ppm Fe sample, which they believe corresponds to the low-temperature saturation concentration. They postulate that the C_p contributions for higher Fe concentrations arise from $ScFe_2$ or Sc_3Fe which is concentrated in the grain boundaries; our samples are single crystals, and, presumably, do not contain grain boundaries. A metallographic and Auger examination of the present samples[32] shows no Fe-bearing inclusions, so the source of the discrepancy is not known. The present results probably are associated with a small concentration of Fe in solid solution.

The "impurity" parameters in Tables I and III were used to calculate the "anomaly" Γ's which are given in Table V. They are large in magnitude and are highly anisotropic, with an anisotropy which is opposite to that of the "spin+*ep*" contribution.

IV. DISCUSSION

The representations used in Figs. 1 (for C_p) and 4 (for α) were chosen to emphasize the relative importance of the electronic (C_p/T or α/T independent of T) and lattice contributions; the different maxima temperatures for Sc and Lu reflect the difference in their Θ_0's. After an adjustment for the disappearance of spin-fluctuation and electron-phonon

TABLE V. Intrinsic Grüneisen parameters Γ for Sc and Lu crystals. The stated "high-T" uncertainties reflect those in $A_0^{\rm adj}$ (Tables II and III). See the text for details.

	Scandium			Lutetium		
	Γ_a	Γ_c	Γ_v	Γ_a	Γ_c	Γ_v
$T=0$ parameters						
Lattice (0 K)	1.26	4.21	2.39	0.66	1.57	1.00
Lattice (300 K)	0.43	2.05	1.00	0.86	0.83	0.85
Electronic	4.11	−4.855	1.10	1.675	6.525	3.48
"High-T" parameters		140–300 K			70–300 K	
Lattice (av)	0.85(1)	0.87(3)	0.90(2)	0.86(2)	1.38(3)	1.06(2)
Electronic	1.0(2)	5.2(6)	2.5(4)	1.9(4)	0.8(6)	1.5(5)
Spin+ep	7.8(3)	−17.9(7)	−0.6(4)	1.1(7)	17.3(12)	7.1(9)
Anomaly	−40	30	−17			

contributions with increasing T, the α anisotropies in Fig. 3 are primarily electronic in origin for Sc, and are associated with the lattice for Lu (see Table V and Fig. 7).

The low-temperature C_p and α data for Sc and Lu give limiting Debye Θ's (Θ_0) which are in reasonable agreement with those obtained in other experiments (Table IV). The $T=0$ lattice Grüneisen parameters (Table V) show that, for each, Θ_0 is more sensitive to c-axis than a-axis strain [Eqs. (6b) and (8)]. These data also give (Table IV) the electronic C_p coefficient γ for each metal (for Sc, γ is 5% greater than a recent calculation[2]) as well as the strain derivatives of $n(\epsilon_F)$, the density of states at the Fermi level [Eqs. (6a) and (8); the $T=0$ "electronic" Γ's in Table V]. These Γ's are quite anisotropic for both Sc and Lu, and for each reflect a combination of a bare density of states contribution and enhancements due to spin fluctuations and the electron-phonon interaction [Eq. (10)].

The decrease of these enhancements with increasing T (Refs. 16 and 17) results in an apparent conflict with the requirements of lattice dynamics if the T dependence of the enhancements is ignored [both the equivalent Θ (Fig. 6) and the lattice Γ's (Fig. 7) should become constant at high T]. The required lattice dynamics consistency can be achieved by appropriately adjusting both γ and the parameters [A_0 in Eq. (1b)] which give the electronic contributions to α. These adjusted parameters, $\gamma_b = C_0^{\rm adj}$ in Tables I and IV and $A_0^{\rm adj}$ in Tables II and III, and the "high-T" Γ's which are calculated using them (Table V), then are characteristic of the high-T bare, unenhanced, density of states.

The resulting γ_b for Sc is approximately 10% larger than that calculated by Götz and Winter,[2] although the sum $\gamma_{\rm spin}+\gamma_{ep}$ $(=\gamma-\gamma_b)$ agrees well. The use of the adjusted coefficients results in high-T lattice Γ's which are isotropic for Sc and quite anisotropic for Lu (Fig. 7 and Table V). The bare electronic Γ's (strain derivatives, Table V) are anisotropic, but not as markedly as those for γ. The most striking result involves the Γ's (strain derivatives) which are associated with the enhancements ($\gamma_{\rm spin}+\gamma_{ep}$) (Table V). These are highly anisotropic, with the largest magnitudes (~17) along the c axis, but (−) for Sc and (+) for Lu. The individual spin and electron-phonon contributions cannot be separated, but the result is an extreme sensitivity of the enhancements to strain along the c axis. A similar anisotropy, but much larger, is found for the Γ's associated with the Fe impurity in the Sc crystal (Table V). An unusual mechanism must exist to cause this effect; the large magnitudes for the anisotropic Γ's suggest tunneling.[25]

Previously, Legvold *et al.*[33] found that the saturated moment of gadolinium-rich alloys was a function of the c/a ratio for these alloys, not the volume, and ascribed this to a sensitivity of the predominantly d-like band near the Fermi level to changes in the c/a ratio, but not to volume changes. The same d-like band is important for Sc,[2] and the present results appear to be consistent with this d-band postulate, although the relationship between the present experiments on pure (nonmagnetic) metals and the magnetic alloys studies is not clear.

In summary, the present results and analysis suggest caution in the separation of C_p and α data into electronic and lattice contributions for metals in which spin-fluctuation and electron-phonon effects are important. The requirement of lattice dynamics consistency not only provides information about the bare density of states at the Fermi level, but, when α and elastic-constant data are available, also shows the complexity of the density of states through the strain derivatives (the Γ's) at that point; the density of states for Sc and Lu, at least, is much more sensitive to uniaxial strain than to volume changes. This is true also for the enhancements, although dependences for the individual contributions from spin fluctuations and the electron-phonon interactions cannot be separated.

ACKNOWLEDGMENTS

K. A. Gschneidner, Jr., kindly provided copies of the thesis of D. K. Thome,[12] which contains a tabulation of the data for the ETP Lu C_p's,[3,7] and of the data for the ETP C_p's of Tsang *et al.*[3,5] Extremely useful conversations with B. N. Harmon are gratefully acknowledged. The single-crystal samples were prepared and characterized in the Materials Preparation Center of the Ames Laboratory. This work was performed at the Ames Laboratory, Iowa State University and was supported by the Director of Energy Research, Office of Basic Science, U.S. Department of Energy under Contract No. W-7405-ENG-82.

APPENDIX: ELASTIC CONSTANTS

Elastic-constant data have been published for both Sc (Ref. 10) and Lu.[8] The elastic constants in each case show a

TABLE VI. The parameters which with Eq. (A1) will reproduce the smooth values for the elastic constants, B_S, and C_p/C_v which were used in the present paper. These parameters, with T in K, will give the elastic constants and B_S in units of 10^{10} Pa (10^{11} d/cm^2); C_p/C_v will be dimensionless.

	M_0	M_1	φ
Sc (Ref. 10, sample IV)			
C_{11}	10.250	-1.98×10^{-3}	200
C_{12}	4.450	3.50×10^{-4}	120
C_{13}	3.000	-2.50×10^{-4}	160
C_{33}	10.170	1.45×10^{-3}	15
C_{44}	2.640	3.50×10^{-4}	15
C_{66}	2.900	-9.80×10^{-4}	106
B_S	5.730	-3.00×10^{-4}	250
C_p/C_v	1.000	4.50×10^{-5}	210
Lu (Ref. 8, sample LuII)			
C_{11}	9.105	-1.98×10^{-3}	110
C_{12}	3.193	5.00×10^{-5}	60
C_{13}	2.865	-5.00×10^{-4}	70
C_{33}	8.400	-1.31×10^{-3}	90
C_{44}	2.916	-9.90×10^{-4}	70
C_{66}	2.953	-9.80×10^{-4}	106
B_S	4.946	-6.70×10^{-4}	35
C_p/C_v	1.000	4.18×10^{-5}	70

significant impurity dependence, with no ''recommended'' results given. Tonnies, Gschneidner, and Spedding[8] give tabulated results for two samples; the data for the ''higher-purity'' LuII has been used for the present calculations. Fisher and Dever[10] give results in graphical form for several samples; the data from their sample IV (ANL) has been (somewhat arbitrarily) selected for use in the present calculations. Since elastic properties can be expected to vary (to first order) with the volume and, hence, with the internal energy of a material, the T-dependent data for each of the elastic constants for Sc and Lu were arbitrarily hand fitted to the form of an Einstein energy function:

$$C_{ij}=M_0+M_1\varphi/\{[\exp(\varphi/T)]-1\}. \tag{A1}$$

The adiabatic bulk modulus B_S, which is calculated from the elastic constants, and the temperature dependence of C_p/C_v [Eq. (5)] also can be represented by this function. Table VI gives the parameters for Eq. (A1) which will represent the experimental C_{ij} data and B_S for Sc and Lu to better than 1% (the temperature dependences are small), and C_p/C_v to better than 0.1%. While M_0 corresponds to the $T=0$ value of the C_{ij}, the magnitudes of M_1 and φ were derived using an *ad hoc* procedure, and have no physical significance whatsoever.

[1] C. A. Swenson, following paper, Phys. Rev. B **53**, 3680 (1996).
[2] W. Götz and H. Winter, J. Phys. Condens. Matter **5**, 1721 (1993).
[3] T.-W. E. Tsang, K. A. Gschneidner, Jr., F. A. Schmidt, and D. K. Thome, Phys. Rev. B **31**, 235 (1985); **31**, 6095(E) (1985).
[4] K. A. Gschneidner, Jr., in *Science and Technology of Rare Earth Materials*, edited by E. C. Subarao and E. C. Wallace (Academic, New York, 1980), p. 25.
[5] T.-W. E. Tsang, K. A. Gschneidner, Jr., and F. A. Schmidt, Solid State Commun. **20**, 737 (1976).
[6] T.-W. E. Tsang and K. A. Gschneidner, Jr., J. Less-Common Met. **80**, 257 (1981).
[7] D. K. Thome, K. A. Gschneidner, Jr., G. S. Mowry, and J. F. Smith, Solid State Commun. **25**, 297 (1978).
[8] J. J. Tonnies, K. A. Gschneidner, Jr., and F. H. Spedding, J. Appl. Phys. **42**, 3275 (1971).
[9] J. D. Greiner, B. J. Beaudry, and J. F. Smith, J. Appl. Phys. **62**, 1220 (1987).
[10] E. S. Fisher and D. Dever (unpublished).
[11] R. G. Leisure, R. B. Schwarz, A. Migliori, and Ming Lei, Phys. Rev. B **48**, 1276 (1993).
[12] David Keith Thome, M.S. thesis, Iowa State University, 1977.
[13] B. C. Gerstein, W. A. Taylor, W. D. Schickell, and F. H. Spedding, J. Chem. Phys. **51**, 2924 (1969).
[14] B. C. Gerstein, W. A. Taylor, W. D. Schickell, and F. H. Spedding, J. Chem. Phys. **54**, 4723 (1971).
[15] J. Pleschiutschnig, O. Blaschko, and W. Reichardt, Phys. Rev. B **41**, 975 (1990).
[16] J. Pleschiutschnig, O. Blaschko, and W. Reichardt, Phys. Rev. B **44**, 6794 (1991).
[17] G. Grimvall, in *The Electron-Phonon Interaction in Metals*, edited by E. P. Wolfarth, Selected Topics in Solid State Physics Vol. 16 (North-Holland, New York, 1981).
[18] K. Ikeda, K. A. Gschneidner, Jr., T.-W. E. Tsang, and F. A. Schmidt, Solid State Commun. **41**, 889 (1982).
[19] R. J. Stierman, K. A. Gschneidner, Jr., T.-W. E. Tsang, F. A. Schmidt, P. Klavins, R. N. Shelton, J. Queen, and S. Legvold, J.

Magn. Magn. Mater. **36**, 249 (1983).
[20] M. S. Anderson and C. A. Swenson, Rev. Sci. Instrum. **49**, 1027 (1978).
[21] J. C. Holste, T. C. Cetas, and C. A. Swenson, Rev. Sci. Instrum. **41**, 670 (1972).
[22] K. A. Gschneidner, Jr., Bull. Alloy Phase Diag. **11**, 216 (1990).
[23] C. A. Swenson, in Thermal Expansion of Solids, edited by R. E. Taylor, CINDAS Data Series on Material Properties Vols. 1–4 (CINDAS/Purdue, West Lafayette, in press), Chap. 8.
[24] T. H. K. Barron and J. A. Morrison, Can. J. Phys. **35**, 799 (1957).
[25] T. H. K. Barron, J. G. Collins, and G. K. White, Adv. Phys. **29**, 609 (1980).
[26] E. S. R. Gopal, *Specific Heats at Low Temperatures* (Plenum, New York, 1966).
[27] G. Grimvall, in *Thermophysical Properties of Materials*, edited by E. P. Wohlfarth, Selected Topics in Solid State Physics Vol. 12 (North-Holland, New York, 1986).
[28] H. Preston-Thomas, Metrologia **27**, 3 (1991); **27**, 107(E) (1991). The official text of the ITS-90 is available from the Bureau International des Poids et Mésures.
[29] R. E. Bedford, M. Durieux, R. Muijlwijk, and C. R. Barber, Metrologia **5**, 47 (1969).
[30] BIPM, *Supplementary information for the ITS-90* (1990). Unpublished, available from the Bureau International des Poids et Mesures.
[31] T. H. Metzger, P. Vajda, and J. N. Daou, Z. Phys. Chem. (Neue Folge) **143**, 129 (1985).
[32] D. T. Peterson (private communication).
[33] S. Legvold, B. N. Harmon, B. J. Beaudry, P. Burgardt, D. R. Younkin, and H. W. White, Phys. Rev. B **16**, 4986 (1977).